Improving the Mechanical Properties of Additively Manufactured Micro-Architected Biodegradable Metals

Li, Yageng; Shi, Jirong; Jahr, Holger; Zhou, Jie; Zadpoor, Amir A.; Wang, Luning

DOI
10.1007/s11837-021-04949-8

Publication date
2021

Document Version
Accepted author manuscript

Published in
JOM

Citation (APA)
Li, Y., Shi, J., Jahr, H., Zhou, J., Zadpoor, A. A., & Wang, L. (2021). Improving the Mechanical Properties of Additively Manufactured Micro-Architected Biodegradable Metals. *JOM*, *73*(12), 4188-4198. https://doi.org/10.1007/s11837-021-04949-8

Review paper

Improving the mechanical properties of additively manufactured micro-architected biodegradable metals

Yageng Li [1#], Jirong Shi [2#], Holger Jahr [3,4], Jie Zhou [5], Amir A. Zadpoor [5], Luning Wang [1*]

[1]*Beijing Advanced Innovation Center for Materials Genome Engineering, School of Materials Science and Engineering, University of Science and Technology Beijing, Beijing, 100083, PR China*

[2]*Department of General Surgery, Peking University First Hospital, Beijing, 100034, PR China*

[3]*Department of Anatomy and Cell Biology, University Hospital RWTH Aachen, Aachen 52074, Germany*

[4]*Department of Orthopedic Surgery, Maastricht UMC+, Maastricht 6202 AZ, The Netherlands*

[5]*Department of Biomechanical Engineering, Delft University of Technology, Delft 2628 CD, The Netherlands*

Keywords: Additive manufacturing; mechanical property; micro-architected; microstructure; geometrical design

[*]Corresponding author; E-mail: luning.wang@ustb.edu.cn

[#]These authors contributed equally to this work.

Abstract

Additively manufactured (AM) micro-architected biodegradable metals offer a unique combination of properties that is ideal for bone regeneration including biocompatibility, a fully interconnected porous structure, and the possibility to fully regenerate bony defects with native tissue upon biodegradation. Currently, the mechanical properties of AM biodegradable porous metals can only match the values of human trabecular bone, hindering their applications for cortical bone regeneration. So far, different approaches have been applied to improve the mechanical properties of AM biodegradable porous metals. Here, we present the state-of-the-art in AM biodegradable porous metals with a focus on the effects of the material composition, geometrical design, AM process, and post-AM treatments on their mechanical properties. We also identify a number of challenges encountered in adopting AM biodegradable porous metals for orthopedic applications from the mechanical viewpoint and suggest some promising areas for future research.

1. INTRODUCTION

Due to the growing and aging population, the world is experiencing rapidly increasing demands for bone implants used in the treatment of osteoarthritis, osteoporotic fractures, and after bone tumor resections or traffic accident-related trauma [1]. Implants for the treatment of critical-sized bony defects are particularly sought after, as such bone defects seriously affect the quality and length of patients' lives. Indeed, the market of bone grafts and substitutes is estimated to be worth $4.15 billion by 2026 [2]. In addition to being biocompatible, an ideal bone substitute should have a fully interconnected porous structure to allow for bone ingrowth, possess bone-mimetic mechanical properties, and gradually degrade in the body after the complete of bone regeneration process [3].

Additive manufacturing (AM) has provided an unprecedented opportunities to develop such porous metallic biomaterials for the treatment of large bone defects [4]. AM can not only customize the macroscale shape of the implants to match the specific anatomy of every individual patient, it can also precisely control the micro-architecture of the fabricated structures, also known as porous structures, so as to mimic the properties of the natural human bone. The mechanical properties, permeability (i.e., mass transport behavior), and the cell behavior can be adjusted by manipulating the design of micro-architected structures [5].

Up till now, many AM porous metallic biomaterials have been investigated, including such bio-inert metals as titanium alloys [6, 7], stainless steel [8], cobalt-chromium alloys [9], and tantalum [10]. However, these materials stay in the body forever, creating a lifelong risk of complications including inflammation and implant-associated infections. Moreover, the presence of a permanently present implant means that the bony defects can never be fully regenerated. Biodegradable metals, such as magnesium, zinc, and iron, have the potential to tackle such problems, as they can gradually degrade in the body [11]. Recently, AM biodegradable porous metals have been developed with fully interconnected porous structures, good biocompatibility, and appropriate biodegradation rates [3]. However, as the research about AM biodegradable porous metals just appeared recently, most of them used pure metal and bending-dominated structures. Meanwhile, AM of magnesium and zinc still remains challenging because of their lower melting points. Currently, the mechanical properties (*e.g.*, yield strength and stiffness) of AM biodegradable porous metals can only match those of the human trabecular bone, which are much lower than the values reported for the human cortical bone [12-14]. Trabecular bone has a compressive yield strength in a range of 2–12 MPa and an elastic modulus value between 0.1 and 5 GPa, while cortical bone has a compressive yield strength between 170 and 193 MPa and an elastic modulus that may be as high as 20 GPa [15]. Moreover, the mechanical properties of AM biodegradable porous metals must be retained at a level high enough to provide mechanical support for 12–24 weeks [11], as biodegradation takes its course. In addition to quasi-static mechanical properties, the fatigue behavior of AM biodegradable porous metals is of particular importance, given the fact that load-bearing orthopedic implants experience millions of loading cycles per year and that biodegradation can deteriorate their fatigue lives [16]. Corrosion fatigue behavior is especially relevant to biodegradable metals, as biodegradation tends to shorten their fatigue lives [17-19].

Therefore, it is important to improve the mechanical properties of AM biodegradable porous metals in order to broaden their applications. As such materials are usually micro-architected, their mechanical properties can be improved both by optimizing the microstructure of the bulk metal they are made of and through an optimized geometrical design. Here, we review the approaches that have so far been applied to improve the mechanical properties of AM micro-architected metallic biomaterials, including alloying, composites, geometrical design, AM process optimization, and post-AM treatment.

2. Effect of material's composition

2.1. Material type

The yield strength and elastic modulus of an AM biodegradable porous metal can be improved by improving the mechanical properties of the material itself. Naturally, biodegradable magnesium, zinc, and iron possess very different mechanical properties. AM pure iron has been reported to reach the highest yield strength (200 – 352 MPa) and elastic modulus (188 – 215 GPa) (Figure 1) [20-22]. AM pure magnesium has a lower yield strength (51 MPa) than the human cortical bone [23], but a similar elastic modulus (27–35 GPa) [24, 25]. While conventionally manufactured pure zinc has an elastic modulus (70–140 GPa) being higher than that of the human cortical bone [26], the reported values of the yield strength and elastic modulus of current AM pure zinc are relatively low (43–150 MPa and 12–32 GPa, respectively) [22, 27-29], probably due to the presence of AM processing defects. In conclusion, only AM pure iron has sufficiently high mechanical properties to allow for the introduction of the appropriate levels of porosity. Since introducing porosity decreases both strength and stiffness, porous biomaterials made of AM pure magnesium and zinc are only appropriate for trabecular bone substitution.

The fatigue behavior of an AM porous metal is largely dependent on the type of the materials they are made of. With similar geometrical designs, AM porous pure iron and zinc have been found to show higher fatigue strengths than the AM porous magnesium alloy, WE43 [30-32]. Remarkably, AM pure iron and zinc do not exhibit catastrophic failures, being similar to the AM porous WE43 magnesium alloy, during fatigue tests, which can be attributed to their highly ductile mechanical behavior.

2.2. ALLOYING

Alloying improves the strength of AM biodegradable porous metals through three mechanisms: solid solution strengthening, second-phase strengthening, and grain refinement strengthening. In solid solution strengthening, considerable atomic size differences between the alloying elements and the host result in lattice distortions and thus lead to a strong strengthening effect. As for second phase strengthening, the degree of hardening relies on the amount, shape, and distribution of the second phase, as well as the interface with the matrix (i.e., coherent, semi-coherent and incoherent). Alloying-induced grain refinement is another way to increase the mechanical properties of AM biodegradable metals and the correlation between the grain size and yield strength is described by the well-known Hall-Petch relationship. The undercooling required for second-phase nucleation and the growth-inhibiting factors are believed to be the critical factors determining the final grain size of AM metals. Taking AM biodegradable magnesium as an example, although the elastic modulus of a Mg-based alloy is relatively insensitive to its chemical composition [33], its yield strength can be significantly improved through proper alloying [34, 35]. For instance, SLM Mg-1Zn has been found to exhibit mechanical properties (ultimate tensile strength: 148 MPa and elongation: 11%) that are even better than the as-cast counterpart [36]. That is most likely caused by the solid solution strengthening of zinc and the uniform distribution of the granular Mg_7Zn_3 eutectic phase as a result of a large deviation from the Mg-Zn phase diagram [36], indicating non-equilibrium solidification and subsequent cooling involved in SLM. The SLM bulk WE43 magnesium alloy can even reach a yield strength of 296.3 ± 2.5 MPa [37], which is comparable to the human cortical bone. In the case of zinc, alloying enables the adjustment of both elastic modulus and yield strength. For instance, SLM Zn-Mg alloys (1, 2, 3 and 4%Mg) have been found to possess significantly increased elastic moduli and yield strengths, as compared to its pure zinc counterpart [28], while the addition of aluminum (1, 3, and 5%) to zinc has been found to decrease the Young's modulus, but increase the yield strength [38], in the case that the materials were in the as-hot-rolled state. AM Zn-Ce alloys (1, 2 and 3% Ce) have been found to exhibit a considerably improved ultimate tensile strengths, as Ce effectively interrupted the grain growth and caused the formation of stable intermetallics, contributing to grain refinement strengthening and Orowan strengthening (Figure 2a) [39]. Similarly, an SLM Fe-Mn scaffold (25% Mn) offer significantly higher yield strengths than the SLM pure iron scaffold (Table 1) [40, 41]. Of course, when choosing the alloying elements for AM biodegradable metals, one should first consider their biocompatibility including elemental toxicity. The degradation of AM biodegradable alloys should generate products that are non-toxic and absorbable by the surrounding tissue or dissolvable for excretion via the kidney renal system [33].

2.3. Composites

One of the attractions of composite materials is improved mechanical properties, including both yield strength and elastic modulus. Particle dispersion strengthening, load transfer, and grain refinement are the key strengthening mechanisms of metal matrix composites [42]. Uniformly distributed fine and hard reinforcing particles in the matrix block the motion of dislocations and thus strengthen the material. Load transfer is another very important strengthening mechanism. The applied stress can be transferred from the matrix to the reinforcing particles, when the bonding between the matrix and the reinforcement is strong enough. The metal matrix is protected due to the higher strength of reinforcing particles. Reinforcing particles can also refine the grains during the solidification process of a composite material by providing heterogeneous nucleation sites, thereby contributing to the strength of the composite. Powder-bed-fusion AM process, especially SLM, makes it convenient to fabricate metal matrix composites by mixing a metal powder with a functional material [43]. For example, reduced graphene oxide (RGO) has been used as the reinforcement to strengthen a Zn scaffold via SLM [44]. Zn powder and RGO flakes were mixed using a ball mill under the protection of argon gas. It was found that the homogeneously distributed RGO contributed to the grain refinement and weakened texture. The RGO-induced grain refinement and the efficient load transfer caused by the huge specific surface area of RGO and the favorable interface bonding improved the mechanical strength of biodegradable Zn (Figure 2b, c). In addition, RGO activated more slip systems in the Zn matrix and thus improved the ductility of the composite. Mesoporous bioglass (MBG) has been also incorporated into a Mg-Zn-Zr alloy (ZK60) through SLM [45]. Although the main purpose was to tailor the biodegradation behavior of the alloy, the resultant SLM ZK60/MBG composite showed a significant improvement in tensile properties, which could be attributed to the reinforcing effect of MBG nanoparticles as well as the grain refinement.

3. EFFECT OF GEOMETRICAL DESIGN

The mechanical properties of micro-architected materials are strongly dependent on their geometrical design, including their porosity and unit cell type. The yield strength and elastic modulus of an AM biodegradable porous metal are directly related to its relative density [46-48]. As for the unit cell type, there are three major types of designs, namely beam-based (*e.g.,* cubic, diamond and dodecahedron) ,sheet-based (*e.g.,* minimal surface designs, including gyroid, Schwartz P (primitive), and Schwartz D (diamond) [4]), and plate-based structures(Figure 3a).

3.1. Beam-based structures

Structures designed using beam-like structural elements can be further divided into bending-dominated and stretch-dominated structures. Generally, bending-dominated structure has higher energy absorption capacities, while a stretch-dominated structures exhibit higher yield strengths [49, 50]. For example, Lietaert et al. [51] studied the mechanical properties of AM porous zinc scaffolds based on the stretch-dominated (*i.e.*, octet truss and kagome) and bending-dominated (*i.e.*, diamond, dodecahedron, and FCC) unit cells. Among those structures, the kagome scaffolds showed the highest plateau stress (15-50 MPa) for the same value of the relative density (0.2-0.3). Surprisingly, however, the strength of the octet truss scaffolds was found to be the lowest (5-30 MPa, 0.3-0.5 relative density), which was explained by the lower manufacturing quality of the octet truss scaffolds, especially the horizontal struts. All the beams of many bending-dominated unit cells, such as those of the diamond unit cell, are tilted at around 35° relative to the building direction. However, stretch-dominated lattice structures usually have at least some struts whose orientation is perpendicular to the building direction, reducing the manufacturing quality of those structures [52]. Moreover, the unit cell type not only determines the mechanical properties of AM porous metals but also decides the failure mode of the scaffolds under compression. For example, it has been shown that the abrupt diagonal shear of SLM Mg lattice can be changed to progressive layer deformation or barreling, depending on the unit cell type [53].

3.2. Sheet-based structures

Triply periodic minimal surface (TPMS) structure constitute an important class of sheet-based structures and are known to possess excellent mechanical properties. Morphologically, TPMS architectures can be categorized into two main types, namely minimal surface network solids and minimal surface sheet solids (Figure 3a) [54]. Al-Ketan et al. [55] investigated the mechanical properties of a wide range of structures, including strut-based, skeletal-TPMS, and sheet-TPMS porous structures. They concluded that sheet-TPMS structures exhibit superior mechanical properties in terms of the elastic modulus. Sheet-based gyroid structures can also sustain relatively higher peak stresses and have higher toughness in comparison with skeletal gyroid structures. Wang et al. [56] used SLM to fabricate porous Mg alloys with different micro architecture designs and found that the gyroid structure has almost two times higher yield strength (16.25 MPa) and Young's modulus (0.76 GPa) than the diamond one (9.4 MPa and 0.47 GPa) with the same porosity. TMPS structure also offer some advantages in terms of AM manufacturability as compared to structures with sharp turns or straight-edged pores and struts, eliminating the issue of thermal deformation caused by long overhangs [57]. In addition, TPMS structures are reported to exhibit favorable fatigue properties because of the continuity and curvature of their structural elements. These removes some of the sources of stress concentrations [58].

3.3. PLATE-BASED STRUCTURES

Another emerging category of micro-architected structure are plate-based lattices, due to their potential to achieve the upper bounds for isotropic elasticity and strain energy storage (i.e., the Hashin-Shtrikman upper bounds) [59]. However, its superior mechanical property comes at the cost of the manufacturing feasibility, as their closed-cell nature obstacles the use of powder-bed AM technique. Duan et al. [60] fabricated the 316L stainless steel lattice from a novel plate-based unit cells with face-holes by SLM, which shows exceptional mechanical performance.

3.4. FUNCTIONALLY GRADED STRUCTURES

Functionally graded materials (FGMs) are characterized by gradual transitions in composition, microstructure, or porosity along at least one direction, leading to functional changes associated with at least one of their properties [61]. AM provides great opportunities for the fabrication of functionally graded porous structures with varied porosity (Figure 3b). The mechanical properties of functionally graded structures could be predicted, based on the weighted average of the mechanical properties of each constituent using the Voight model [62]. It can then be imagined that the yield strength and the elastic modulus of FGM fall within the values corresponding to the the highest and lowest porosities present in the structure. Maskery et al. [63] found that graded structures underwent collapse in a layer-by-layer sequence during compression test, suppressing the formation of diagonal shear bands, which, makes the deformation and energy absorption profiles of functionally graded structures more predictable than uniform ones with the same mean relative density. Functionally graded structures have also been shown to improve the fatigue performance of AM biodegradable porous metals. For example, for the diamond unit cell, fatigue cracks tend to initiate at the junctions between the two struts where tensile stress concentration occurs under compression [30-32]. Li et al. [32] found that graded structure designs could increase the fatigue strength of SLM porous zinc. Similar results have been obtained for AM functionally graded porous Ti-6Al-4V [64].

4. EFFECTS OF AM PROCESS PARAMETERS

4.1. DENSITY

The mechanical properties of porous metals are largely determined by the specific AM process applied during their fabrication. SLM process parameters, such as laser power, scanning speed, hatch spacing, and layer thickness, have significant impacts on the resulting relative density of the as-built specimens [65]. Internal pores inside the struts of a scaffold can not only deteriorate the static mechanical properties of AM porous metals but also act as crack initiation sites, shortening their fatigue life as well [66]. The most importance factors that affect the density of SLM porous metals can all be related to the laser energy density:

$$Ev = P/(V \bullet Hs \bullet Ds) \text{ J/mm}^3$$

where Ev is the laser energy density, P is the laser power, V is the scanning speed, Hs is the hatching space, and Ds is the layer thickness. Initially, densification increases with increasing laser energy density to melt all powder particles and then decreases because excessive laser energy leads to an unstable keyhole and too strong evaporation. As observed in the case of SLM AZ91 [67], increasing the energy density from 66 J/mm^3 to 167 J/mm^3 can improve the densification process during SLM, thereby enhancing the mechanical properties of the resulting material. However, increasing the energy density further to above 214 J/mm^3 caused very high temperatures in the molten pool and serious evaporation, leading to a failed SLM process. A similar trend has been reported for SLM Zn as well [27] (Figure 4a). In the case of porous structures, the scanning strategy highly affects the densification of the struts. Demir et al. [68] found that concentric scanning is more suitable for fabricating struts than linear hatching for SLM CoCr stents. The AM process optimization should then be adapted according to the different micro-architectures.

4.2. MICROSTRUCTURES

Due to rapid solidification, SLM biodegradable porous metals normally have much finer grain sizes than the conventionally manufactured counterparts, which can improve the strengths of those materials, according to the Hall-Patch relationship [12-14]. For biodegradable alloys, segregation of alloying elements takes place within a small melting pool. The chemical composition is then more uniform throughout the SLM metals, resulting in higher strength than cast counterparts. Different AM process parameters lead to different grain sizes and grain orientations, both of which can affect the mechanical properties of AM biodegradable porous metals [69]. A lower laser energy density during SLM typically results in a finer microstructure due to a high cooling rate. In contrast, a higher laser energy density can lead to relatively equivalent cooling rates in each directions of melt pool during solidification and thus creating the kinetic conditions for equiaxed growth of grains during SLM. A further increase in laser energy density may cause the coarsening of grains. Qin et al. [70] found that increasing the scanning speed from 300 to 700 mm/s resulted in finer grains, irregular grain morphology, and a weaker grain texture, which enhanced the strength and ductility of SLM pure Zn (Figure 4b). Owing to the layer-by-layer nature of fabrication process, the building orientation of the specimens affects the resulting mechanical properties as well. For example, vertically built SLM Zn tensile specimens showed higher strength and ductility compared with horizontally built specimens, implying the strong anisotropy of the mechanical properties [70]. As each design has a different set of the orientation angles of structural elements, the effects of the anisotropic microstructure within the micro-architected structures on the mechanical properties of AM porous biodegradable metals need to be further studied

5. Effect of post-AM treatments

5.1. Heat-treatment

As discussed above, AM metals normally have anisotropic microstructures, internal pores, and residual stresses, which can deteriorate their ductility and fatigue strength. Heat treatment can be used to mitigate or eliminate such detrimental effects [66]. In general, post-AM heat treatments that can increase the ductility of the AM material are also beneficial in terms of the fatigue strength [71]. For example, hot isostatic pressing

(HIP) is a powerful high pressure heat treatment aimed at closing internal pores and improving the microstructure of parts [72]. HIP has been used to significantly improve the ductility and fatigue resistance of SLM/EBM porous Ti-6Al-4V [52, 73]. It is then interesting to study the effect of HIP on the mechanical properties of AM biodegradable porous metals. Annealing is an effective heat treatment to eliminate residual stress in AM metals. The compressive strength of SLM WE43 scaffolds was shown to decrease after annealing [74], while SLM iron scaffolds exhibited a higher yield strength after vacuum annealing, as a result of grain refinement caused by the residual stress as the driving force for recrystallization (Figure 5a) [20]. For some biodegradable alloys, the solution treatment can be followed by an ageing treatment to promote precipitation hardening and improve the mechanical properties. Chen et al. [75] reported that the strength of the ZK60 alloy was improved by applying the T5 treatment due to the formation of small and uniformly distributed MgZn phase particles. Thus, special heat treatment procedures can be developed to improve the mechanical properties of AM biodegradable porous metals.

5.2. SURFACE TREATMENT

Adherent powder particles are typically present on the surface of as-built AM biodegradable porous metals. Such sources of surface roughness directly affect the fatigue strength of AM porous metals, given that local roughness effectively acts similar to notches promoting crack initiation [76]. Therefore, chemical etching or sandblasting has been used to polish the surface of AM biodegradable scaffolds [13, 14, 27, 77].

Chemical etching showed minimal detrimental effects on the yield strength or stiffness of AM biodegradable scaffolds (Figure 5b) [13, 14]. Since sandblasting has been found to improve the fatigue resistance of AM porous titanium because of eliminated surface imperfections and induced favorable compressive stress [7], it could be applied to improve the fatigue resistance of AM biodegradable porous metals as well. Although coatings on porous biomaterials are normally not aimed for improving mechanical properties, it is interesting to study the effect of bio-functional coating as well. Plasma electrolytic oxidation (PEO) has been shown to increase the compressive strength of SLM WE43 scaffolds [74]. Electrodeposition of Zn on biodegradable porous Fe core has also been found to increase the yield strength and modulus of the scaffold [78].

6. DISCUSSION AND FUTURE RESEARCH

To date, most AM biodegradable porous metals have shown lower mechanical properties than human cortical bone, making them more suitable for trabecular bone substitution. According to what was discussed above, there are several approaches that can be adopted to improve the mechanical properties of AM biodegradable porous metals to further broaden their scope of applications as bone substitutes.

First, from the material's point of view, commonly used strengthening methods such as alloying and the design of metal matrix composites can be used for increasing the mechanical properties of the bulk material from which the micro-architected porous structures are made. The strengthening mechanisms through alloying normally include grain boundary strengthening, solid solution strengthening, precipitation strengthening, and dispersion strengthening. According to the Hall-Petch relationship, the yield strength is inversely related to the grain size. In the case of SLM, the grain size of biodegradable porous metals can be adjusted by controlling the thermal history of each layer, alloying elements, and reinforcing particles. In solid solution strengthening, alloying can be used to introduce solute atoms that can cause lattice distortions that hinder dislocation motion. Precipitation strengthening happens when the concentration of an alloying element is beyond its solid solubility, promoting the formation of second-phase particles. Both second-phase particles and reinforcing particles can work as pining points for dislocations. Via these rules, high-strength alloys or composites can be designed to improve the mechanical properties of AM biodegradable porous metals. Secondly, from a geometrical point of view, most of the current AM biodegradable porous metals are designed using bending-dominated unit cells (*e.g.*, the diamond unit cell). Micro-architected structures based on stretch-dominated unit cells or minimal surfaces or plate-based unit cells should be applied to improve the strength and stiffness of AM biodegradable porous metals. Functionally graded structures that combine different unit cell types and unit cell sizes could be developed to avoid abrupt failure and achieve better fatigue performance. Considering the fact that it is very demanding to replicate the complex structure of the human bone [79], it is important to build a database for the mechanical properties of the different micro-architected structures and apply machine learning techniques to relate the relevant aspects of the geometry design and the mechanical properties of the resulting objects.

In addition to the abovementioned factors, it is important to minimize the manufacturing defects present in the state-of-the-art AM biodegradable metals through

AM process optimization, post-AM heat treatments, and post-AM surface treatments. However, identifying the optimal process parameters remains a significant challenge given that the quality of SLM biodegradable metals is very sensitive to many factors, including the powder characteristics, the geometry of the object, and the laser parameters [80]. Machine learning could be used in the future to predict the process-property relationships and effectively identify the defects [81, 82].

Finally, AM biodegradable porous implants should be designed not only with the aim of achieving initially bone-mimicking mechanical properties but also with a proper consideration on how those properties change with time as the biodegradation and bone regeneration processes progress. The mechanical design of AM biodegradable porous metals, therefore, requires a much more sophisticated approach than simple mechanical testing, according to the standard procedures that are often used in the development of biomaterials. The studies addressing the corrosion fatigue behavior of AM biodegradable porous metals are still limited in number and scope. As far as mechanical testing is concerned, the creep and aging of AM biodegradable metals and their relationship with the time-dependent performance of orthopedic implants need to be further investigated. Moreover, different loading regimes, such as compression-tension, tension-tension, bending, and torsion, should be applied to AM biodegradable porous metals, depending on the loading condition during the practical use.

CONFLICT OF INTEREST

The authors declare that they have no conflict of interest.

References

[1] G.L. Koons, M. Diba, A.G. Mikos, Materials design for bone-tissue engineering, Nat. Rev. Mater. 5(8) (2020) 584-603.

[2] H. Jahr, Y. Li, J. Zhou, A.A. Zadpoor, K.-U. Schröder, Additively manufactured absorbable porous metal implants – processing, alloying and corrosion behavior, Front. Mater. 8(111) (2021).

[3] Y. Li, H. Jahr, J. Zhou, A.A. Zadpoor, Additively manufactured biodegradable porous metals, Acta Biomater. 115 (2020) 29-50.

[4] A.A. Zadpoor, Additively manufactured porous metallic biomaterials, J. Mater. Chem. B 7(26) (2019) 4088-4117.

[5] A.A. Zadpoor, Meta-biomaterials, Biomater. Sci. 8(1) (2020) 18-38.

[6] S.M. Ahmadi, R. Hedayati, Y. Li, K. Lietaert, N. Tümer, A. Fatemi, C.D. Rans, B. Pouran, H. Weinans, A.A. Zadpoor, Fatigue performance of additively manufactured meta-biomaterials: The effects of topology and material type, Acta Biomater. 65 (2018) 292-304.

[7] S.M. Ahmadi, R. Kumar, E.V. Borisov, R. Petrov, S. Leeflang, Y. Li, N. Tümer, R. Huizenga, C. Ayas, A.A. Zadpoor, V.A. Popovich, From microstructural design to surface engineering: A tailored approach for improving fatigue life of additively manufactured meta-biomaterials, Acta Biomater. 83 (2019) 153-166.

[8] C. Yan, L. Hao, A. Hussein, P. Young, D. Raymont, Advanced lightweight 316L stainless steel cellular lattice structures fabricated via selective laser melting, Mater. Des. 55 (2014) 533-541.

[9] R. Hedayati, S.M. Ahmadi, K. Lietaert, B. Pouran, Y. Li, H. Weinans, C.D. Rans, A.A. Zadpoor, Isolated and modulated effects of topology and material type on the mechanical properties of additively manufactured porous biomaterials, J. Mech. Behav. Biomed. Mater. 79 (2018) 254-263.

[10] R. Wauthle, J. van der Stok, S. Amin Yavari, J. Van Humbeeck, J.-P. Kruth, A.A. Zadpoor, H. Weinans, M. Mulier, J. Schrooten, Additively manufactured porous tantalum implants, Acta Biomater. 14 (2015) 217-225.

[11] Y.F. Zheng, X.N. Gu, F. Witte, Biodegradable metals, Mater. Sci. Eng. R Rep. 77 (2014) 1-34.

[12] Y. Li, P. Pavanram, J. Zhou, K. Lietaert, P. Taheri, W. Li, H. San, M.A. Leeflang, J.M.C. Mol, H. Jahr, A.A. Zadpoor, Additively manufactured biodegradable porous zinc, Acta Biomater. 101 (2020) 609-623.

[13] Y. Li, J. Zhou, P. Pavanram, M.A. Leeflang, L.I. Fockaert, B. Pouran, N. Tümer, K.U. Schröder, J.M.C. Mol, H. Weinans, H. Jahr, A.A. Zadpoor, Additively manufactured biodegradable porous magnesium, Acta Biomater. 67 (2018) 378-392.

[14] Y. Li, H. Jahr, K. Lietaert, P. Pavanram, A. Yilmaz, L.I. Fockaert, M.A. Leeflang, B. Pouran, Y. Gonzalez-Garcia, H. Weinans, J.M.C. Mol, J. Zhou, A.A. Zadpoor, Additively manufactured biodegradable porous iron, Acta Biomater. 77 (2018) 380-393.

[15] S. Wu, X. Liu, K.W.K. Yeung, C. Liu, X. Yang, Biomimetic porous scaffolds for bone tissue engineering, Mater. Sci. Eng. R Rep. 80 (2014) 1-36.

[16] F. Bobbert, K. Lietaert, A. Eftekhari, B. Pouran, S. Ahmadi, H. Weinans, A. Zadpoor, Additively manufactured metallic porous biomaterials based on minimal surfaces: A unique combination of topological, mechanical, and mass transport properties, Acta Biomater. 53 (2017) 572-584.
[17] D. Bian, W. Zhou, Y. Liu, N. Li, Y. Zheng, Z. Sun, Fatigue behaviors of HP-Mg, Mg–Ca and Mg–Zn–Ca biodegradable metals in air and simulated body fluid, Acta Biomater. 41 (2016) 351-360.
[18] S. Jafari, R.K. Singh Raman, C.H.J. Davies, Corrosion fatigue of a magnesium alloy in modified simulated body fluid, Eng. Fract. Mech. 137 (2015) 2-11.
[19] M.P. Sealy, Y.B. Guo, R.C. Caslaru, J. Sharkins, D. Feldman, Fatigue performance of biodegradable magnesium–calcium alloy processed by laser shock peening for orthopedic implants, Int. J. Fatigue 82 (2016) 428-436.
[20] B. Song, S. Dong, Q. Liu, H. Liao, C. Coddet, Vacuum heat treatment of iron parts produced by selective laser melting: Microstructure, residual stress and tensile behavior, Mater. Des. 54 (2014) 727-733.
[21] B. Song, S. Dong, S. Deng, H. Liao, C. Coddet, Microstructure and tensile properties of iron parts fabricated by selective laser melting, Opt. Laser Technol. 56 (2014) 451-460.
[22] M. Montani, A.G. Demir, E. Mostaed, M. Vedani, B. Previtali, Processability of pure Zn and pure Fe by SLM for biodegradable metallic implant manufacturing, Rapid Prototyp. J. 23(3) (2017) 514-523.
[23] Y. Zhou, P. Wu, Y. Yang, D. Gao, P. Feng, C. Gao, H. Wu, Y. Liu, H. Bian, C. Shuai, The microstructure, mechanical properties and degradation behavior of laser-melted MgSn alloys, J. Alloys Compd. 687 (2016) 109-114.
[24] C.C. Ng, M.M. Savalani, M.L. Lau, H.C. Man, Microstructure and mechanical properties of selective laser melted magnesium, Appl. Surf. Sci. 257(17) (2011) 7447-7454.
[25] C.C. Ng, M. Savalani, H.C. Man, Fabrication of magnesium using selective laser melting technique, Rapid Prototyp. J. 17(6) (2011) 479-490.
[26] M. Krystýnová, P. Doležal, S. Fintová, M. Březina, J. Zapletal, J. Wasserbauer, Preparation and characterization of zinc materials prepared by powder metallurgy, Metals 7(10) (2017) 396.
[27] P. Wen, M. Voshage, L. Jauer, Y. Chen, Y. Qin, R. Poprawe, J.H. Schleifenbaum, Laser additive manufacturing of Zn metal parts for biodegradable applications: Processing, formation quality and mechanical properties, Mater. Des. 155 (2018) 36-45.
[28] Y. Yang, F. Yuan, C. Gao, P. Feng, L. Xue, S. He, C. Shuai, A combined strategy to enhance the properties of Zn by laser rapid solidification and laser alloying, J. Mech. Behav. Biomed. Mater. 82 (2018) 51-60.
[29] C. Shuai, L. Xue, C. Gao, Y. Yang, S. Peng, Y. Zhang, Selective laser melting of Zn–Ag alloys for bone repair: microstructure, mechanical properties and degradation behaviour, Virtual Phys. Prototyp. 13(3) (2018) 146-154.
[30] Y. Li, H. Jahr, X.Y. Zhang, M.A. Leeflang, W. Li, B. Pouran, F.D. Tichelaar, H. Weinans, J. Zhou, A.A. Zadpoor, Biodegradation-affected fatigue behavior of additively manufactured porous magnesium, Addit. Manuf. 28 (2019) 299-311.

[31] Y. Li, K. Lietaert, W. Li, X.Y. Zhang, M.A. Leeflang, J. Zhou, A.A. Zadpoor, Corrosion fatigue behavior of additively manufactured biodegradable porous iron, Corros. Sci. 156 (2019) 106-116.
[32] Y. Li, W. Li, F.S.L. Bobbert, K. Lietaert, J.H. Dong, M.A. Leeflang, J. Zhou, A.A. Zadpoor, Corrosion fatigue behavior of additively manufactured biodegradable porous zinc, Acta Biomater. 106 (2020) 439-449.
[33] Y. Chen, Z. Xu, C. Smith, J. Sankar, Recent advances on the development of magnesium alloys for biodegradable implants, Acta Biomater. 10(11) (2014) 4561-4573.
[34] C. Shuai, L. Liu, M. Zhao, P. Feng, Y. Yang, W. Guo, C. Gao, F. Yuan, Microstructure, biodegradation, antibacterial and mechanical properties of ZK60-Cu alloys prepared by selective laser melting technique, J. Mater. Sci. Technol. 34(10) (2018) 1944-1952.
[35] Y. Qin, P. Wen, M. Voshage, Y. Chen, P.G. Schückler, L. Jauer, D. Xia, H. Guo, Y. Zheng, J.H. Schleifenbaum, Additive manufacturing of biodegradable Zn-xWE43 porous scaffolds: Formation quality, microstructure and mechanical properties, Mater. Des. 181 (2019) 107937.
[36] K. Wei, X. Zeng, Z. Wang, J. Deng, M. Liu, G. Huang, X. Yuan, Selective laser melting of Mg-Zn binary alloys: Effects of Zn content on densification behavior, microstructure, and mechanical property, Mater. Sci. Eng., A 756 (2019) 226-236.
[37] N.A. Zumdick, L. Jauer, L.C. Kersting, T.N. Kutz, J.H. Schleifenbaum, D. Zander, Additive manufactured WE43 magnesium: A comparative study of the microstructure and mechanical properties with those of powder extruded and as-cast WE43, Mater. Charact. 147 (2019) 384-397.
[38] P.K. Bowen, J.-M. Seitz, R.J. Guillory II, J.P. Braykovich, S. Zhao, J. Goldman, J.W. Drelich, Evaluation of wrought Zn–Al alloys (1, 3, and 5 wt % Al) through mechanical and in vivo testing for stent applications, J. Biomed. Mater. Res. B Appl. Biomater. 106(1) (2018) 245-258.
[39] Y. Yang, M. Yang, C. He, F. Qi, D. Wang, S. Peng, C. Shuai, Rare earth improves strength and creep resistance of additively manufactured Zn implants, Compos. B. Eng. 216 (2021) 108882.
[40] D. Carluccio, C. Xu, J. Venezuela, Y. Cao, D. Kent, M. Bermingham, A.G. Demir, B. Previtali, Q. Ye, M. Dargusch, Additively manufactured iron-manganese for biodegradable porous load-bearing bone scaffold applications, Acta Biomater. 103 (2020) 346-360.
[41] C. Shuai, W. Yang, Y. Yang, H. Pan, C. He, F. Qi, D. Xie, H. Liang, Selective laser melted Fe-Mn bone scaffold: microstructure, corrosion behavior and cell response, Mater. Res. Express 7(1) (2020) 015404.
[42] H.Z. Ye, X.Y. Liu, Review of recent studies in magnesium matrix composites, J. Mater. Sci. 39(20) (2004) 6153-6171.
[43] J. Wu, L. Wang, Selective laser melting manufactured CNTs/AZ31B composites: Heat transfer and vaporized porosity evolution, J. Mater. Res. 33(18) (2018) 2752-2762.
[44] Y. Yang, Y. Cheng, S. Peng, L. Xu, C. He, F. Qi, M. Zhao, C. Shuai, Microstructure evolution and texture tailoring of reduced graphene oxide reinforced Zn scaffold, Bioact. Mater. 6(5) (2021) 1230-1241.

[45] Y. Yang, C. Lu, L. Shen, Z. Zhao, S. Peng, C. Shuai, In-situ deposition of apatite layer to protect Mg-based composite fabricated via laser additive manufacturing, J. Magnes. Alloy. (2021).
[46] Y. Li, H. Jahr, P. Pavanram, F.S.L. Bobbert, U. Puggi, X.Y. Zhang, B. Pouran, M.A. Leeflang, H. Weinans, J. Zhou, A.A. Zadpoor, Additively manufactured functionally graded biodegradable porous iron, Acta Biomater. 96 (2019) 646-661.
[47] Y. Li, P. Pavanram, J. Zhou, K. Lietaert, F.S.L. Bobbert, Y. Kubo, M.A. Leeflang, H. Jahr, A.A. Zadpoor, Additively manufactured functionally graded biodegradable porous zinc, Biomater. Sci. 8(9) (2020) 2404-2419.
[48] Y. Nie, G. Chen, H. Peng, S. Tang, Z. Zhou, F. Pei, B. Shen, In vitro and 48 weeks in vivo performances of 3D printed porous Fe-30Mn biodegradable scaffolds, Acta Biomater. 121 (2021) 724-740.
[49] V.S. Deshpande, M.F. Ashby, N.A. Fleck, Foam topology: bending versus stretching dominated architectures, Acta Mater. 49(6) (2001) 1035-1040.
[50] A.A. Zadpoor, Mechanical performance of additively manufactured meta-biomaterials, Acta Biomater. 85 (2019) 41-59.
[51] K. Lietaert, A.A. Zadpoor, M. Sonnaert, J. Schrooten, L. Weber, A. Mortensen, J. Vleugels, Mechanical properties and cytocompatibility of dense and porous Zn produced by laser powder bed fusion for biodegradable implant applications, Acta Biomater. 110 (2020) 289-302.
[52] R. Wauthle, B. Vrancken, B. Beynaerts, K. Jorissen, J. Schrooten, J.-P. Kruth, J. Van Humbeeck, Effects of build orientation and heat treatment on the microstructure and mechanical properties of selective laser melted Ti6Al4V lattice structures, Addit. Manuf. 5 (2015) 77-84.
[53] H. Hyer, L. Zhou, Q. Liu, D. Wu, S. Song, Y. Bai, B. McWilliams, K. Cho, Y. Sohn, High strength WE43 microlattice structures additively manufactured by laser powder bed fusion, Materialia 16 (2021) 101067.
[54] J. Ding, Q. Zou, S. Qu, P. Bartolo, X. Song, C.C.L. Wang, STL-free design and manufacturing paradigm for high-precision powder bed fusion, CIRP Ann. Manuf. Technol. (2021).
[55] O. Al-Ketan, R. Rowshan, R.K. Abu Al-Rub, Topology-mechanical property relationship of 3D printed strut, skeletal, and sheet based periodic metallic cellular materials, Addit. Manuf. 19 (2018) 167-183.
[56] Y. Wang, P. Fu, N. Wang, L. Peng, B. Kang, H. Zeng, G. Yuan, W. Ding, Challenges and solutions for the additive manufacturing of biodegradable magnesium implants, Engineering 6(11) (2020) 1267-1275.
[57] L. Yuan, S. Ding, C. Wen, Additive manufacturing technology for porous metal implant applications and triple minimal surface structures: A review, Bioact. Mater. 4 (2019) 56-70.
[58] M. Speirs, B. Van Hooreweder, J. Van Humbeeck, J.P. Kruth, Fatigue behaviour of NiTi shape memory alloy scaffolds produced by SLM, a unit cell design comparison, J. Mech. Behav. Biomed. Mater. 70 (2017) 53-59.
[59] M.-T. Hsieh, C.S. Ha, Z. Xu, S. Kim, H.F. Wu, V. Kunc, X. Zheng, Stiff and strong, lightweight bi-material sandwich plate-lattices with enhanced energy absorption, J. Mater. Res. (2021).

[60] S. Duan, W. Wen, D. Fang, Additively-manufactured anisotropic and isotropic 3D plate-lattice materials for enhanced mechanical performance: Simulations & experiments, Acta Mater. 199 (2020) 397-412.
[61] C. Zhang, F. Chen, Z. Huang, M. Jia, G. Chen, Y. Ye, Y. Lin, W. Liu, B. Chen, Q. Shen, L. Zhang, E.J. Lavernia, Additive manufacturing of functionally graded materials: A review, Mater. Sci. Eng., A 764 (2019) 138209.
[62] X.-Y. Zhang, G. Fang, S. Leeflang, A.A. Zadpoor, J. Zhou, Topological design, permeability and mechanical behavior of additively manufactured functionally graded porous metallic biomaterials, Acta Biomater. 84 (2019) 437-452.
[63] I. Maskery, N.T. Aboulkhair, A.O. Aremu, C.J. Tuck, I.A. Ashcroft, R.D. Wildman, R.J.M. Hague, A mechanical property evaluation of graded density Al-Si10-Mg lattice structures manufactured by selective laser melting, Mater. Sci. Eng., A 670 (2016) 264-274.
[64] S. Zhao, S.J. Li, S.G. Wang, W.T. Hou, Y. Li, L.C. Zhang, Y.L. Hao, R. Yang, R.D.K. Misra, L.E. Murr, Compressive and fatigue behavior of functionally graded Ti-6Al-4V meshes fabricated by electron beam melting, Acta Mater. 150 (2018) 1-15.
[65] T. Kurzynowski, A. Pawlak, E. Chlebus, Processing of magnesium alloy by selective laser melting, Proceedings of the 14th International Scientific Conference: Computer Aided Engineering, Springer International Publishing, Cham, 2019, pp. 411-418.
[66] M. Benedetti, A. du Plessis, R.O. Ritchie, M. Dallago, S.M.J. Razavi, F. Berto, Architected cellular materials: A review on their mechanical properties towards fatigue-tolerant design and fabrication, Mater. Sci. Eng. R Rep. 144 (2021) 100606.
[67] K. Wei, M. Gao, Z. Wang, X. Zeng, Effect of energy input on formability, microstructure and mechanical properties of selective laser melted AZ91D magnesium alloy, Mater. Sci. Eng., A 611 (2014) 212-222.
[68] A.G. Demir, B. Previtali, Additive manufacturing of cardiovascular CoCr stents by selective laser melting, Mater. Des. 119 (2017) 338-350.
[69] V. Manakari, G. Parande, M. Gupta, Selective laser melting of magnesium and magnesium alloy powders: a review, Metals 7(1) (2016) 2.
[70] Y. Qin, P. Wen, D. Xia, H. Guo, M. Voshage, L. Jauer, Y. Zheng, J.H. Schleifenbaum, Y. Tian, Effect of grain structure on the mechanical properties and in vitro corrosion behavior of additively manufactured pure Zn, Addit. Manuf. 33 (2020) 101134.
[71] S. Leuders, M. Thöne, A. Riemer, T. Niendorf, T. Tröster, H.A. Richard, H.J. Maier, On the mechanical behaviour of titanium alloy TiAl6V4 manufactured by selective laser melting: Fatigue resistance and crack growth performance, Int. J. Fatigue 48 (2013) 300-307.
[72] S.L. Lu, H.P. Tang, Y.P. Ning, N. Liu, D.H. StJohn, M. Qian, Microstructure and mechanical properties of long Ti-6Al-4V rods additively manufactured by selective electron beam melting out of a deep powder bed and the effect of subsequent hot isostatic pressing, Metall. Mater. Trans. A 46(9) (2015) 3824-3834.
[73] M.-W. Wu, J.-K. Chen, B.-H. Lin, P.-H. Chiang, Improved fatigue endurance ratio of additive manufactured Ti-6Al-4V lattice by hot isostatic pressing, Mater. Des. 134 (2017) 163-170.
[74] A. Kopp, T. Derra, M. Müther, L. Jauer, J.H. Schleifenbaum, M. Voshage, O. Jung, R. Smeets, N. Kröger, Influence of design and postprocessing parameters on the degradation

behavior and mechanical properties of additively manufactured magnesium scaffolds, Acta Biomater. 98 (2019) 23-35.
[75] J. Chen, L. Tan, K. Yang, Effect of heat treatment on mechanical and biodegradable properties of an extruded ZK60 alloy, Bioact. Mater. 2(1) (2017) 19-26.
[76] K. Solberg, F. Berto, A diagram for capturing and predicting failure locations in notch geometries produced by additive manufacturing, Int. J. Fatigue 134 (2020) 105428.
[77] P. Wen, L. Jauer, M. Voshage, Y. Chen, R. Poprawe, J.H. Schleifenbaum, Densification behavior of pure Zn metal parts produced by selective laser melting for manufacturing biodegradable implants, J. Mater. Process. Technol. 258 (2018) 128-137.
[78] J. He, J. Fang, P. Wei, Y. Li, H. Guo, Q. Mei, F. Ren, Cancellous bone-like porous Fe@Zn scaffolds with core-shell-structured skeletons for biodegradable bone implants, Acta Biomater. 121 (2021) 665-681.
[79] X. Wang, S. Xu, S. Zhou, W. Xu, M. Leary, P. Choong, M. Qian, M. Brandt, Y.M. Xie, Topological design and additive manufacturing of porous metals for bone scaffolds and orthopaedic implants: A review, Biomaterials 83 (2016) 127-141.
[80] B. Yuan, G.M. Guss, A.C. Wilson, S.P. Hau-Riege, P.J. DePond, S. McMains, M.J. Matthews, B. Giera, Machine-learning-based monitoring of laser powder bed fusion, Adv. Mater. Technol. 3(12) (2018) 1800136.
[81] B. Kappes, S. Moorthy, D. Drake, H. Geerlings, A. Stebner, Machine learning to optimize additive manufacturing parameters for laser powder bed fusion of inconel 718, Proceedings of the 9th International Symposium on Superalloy 718 & Derivatives: Energy, Aerospace, and Industrial Applications, Springer International Publishing, Cham, 2018, pp. 595-610.
[82] A. Caggiano, J. Zhang, V. Alfieri, F. Caiazzo, R. Gao, R. Teti, Machine learning-based image processing for on-line defect recognition in additive manufacturing, CIRP Ann. Manuf. Technol. 68(1) (2019) 451-454.
[83] C. Shuai, Y. Cheng, Y. Yang, S. Peng, W. Yang, F. Qi, Laser additive manufacturing of Zn-2Al part for bone repair: Formability, microstructure and properties, J. Alloys Compd. 798 (2019) 606-615.

FIGURE CAPTIONS

Figure 1. The mechanical properties of AM biodegradable metals [13, 14, 20-23, 27-29, 34-37, 40, 41, 43, 46, 47, 56, 65, 67, 70, 74, 77, 83] (a) the yield strength and (b) elastic modulus of bulk metals as well as (c) the yield strength and (d) elastic modulus of porous metals.

Figure 2. The microstructures of AM biodegradable porous alloys and composites (a) the inverse pole figures of SLM Zn and Zn-Ce parts [39], (b) TEM images showing the interface bonding of RGO in the Zn matrix [44], and (c) the possible strengthening mechanisms of RGO, which could effectively limit crack propagation in the composite. Reprinted with permission from reference [39].

Figure 3. Micro-architectured structures: (a) different types of unit cell, and (b) the designs of AM functionally graded biodegradable porous iron [46].

Figure 4. The effects of processing parameters on the quality of AM biodegradable metals (a) relationship between the density of AM pure zinc and the energy density related to scanning speed and power input [27], and (b) the EBSD orientation maps of SLM pure zinc corresponding to different scanning speeds [70]. Reprinted with permission from reference [27] [70].

Figure 5. Post treatments for AM biodegradable metals: (a) optical microscope observation from the side view and from the top view of the as-fabricated iron cubes (1 and 2) and of the annealed iron cubes (3 and 4) [20], and (b) the surface quality of AM

biodegradable porous magnesium alloy WE43 before and after chemical polishing. Reprinted with permission from reference [20].

Figure 1

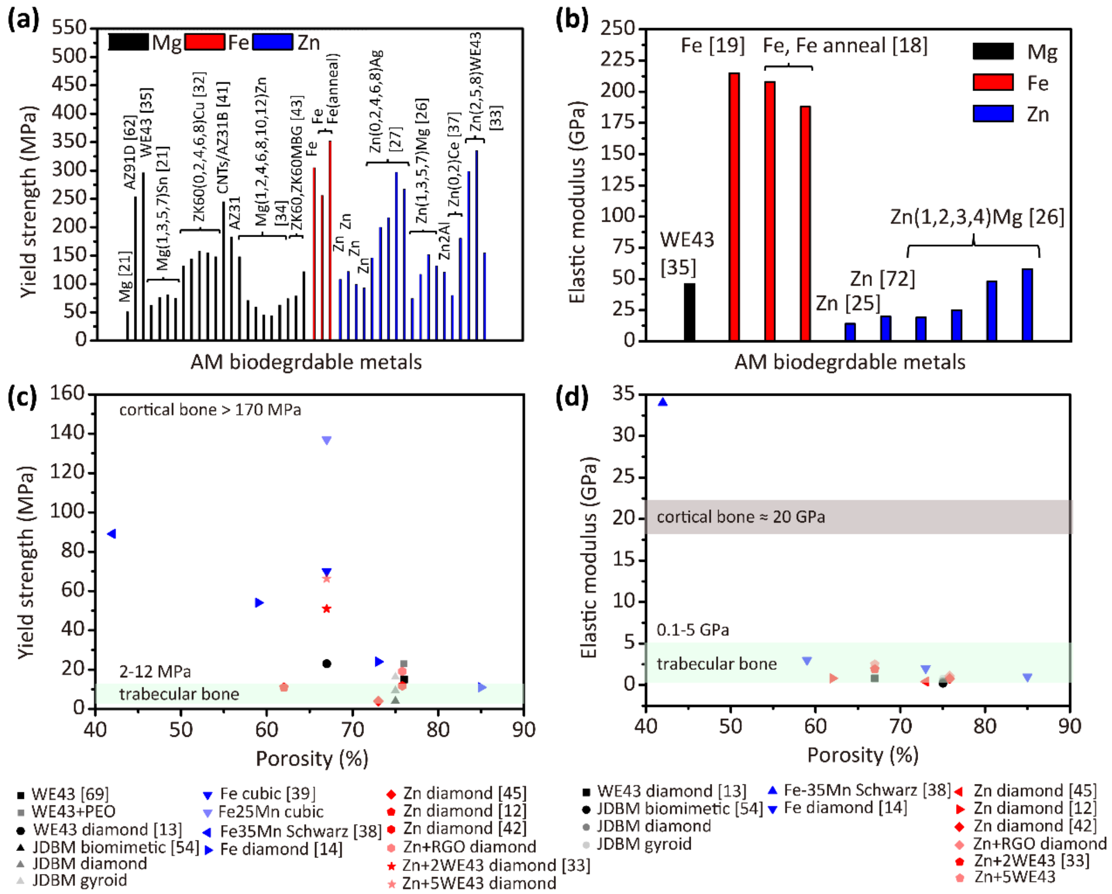

(a)
Yield strength (MPa)
AM biodegrdable metals
Mg
Fe
Zn
(b)
Elastic modulus (GPa)
AM biodegrdable metals
Fe [19]
Fe, Fe anneal [18]
WE43 [35]
Zn(1,2,3,4)Mg [26]
Zn [72]
Zn [25]
(c)
Yield strength (MPa)
Porosity (%)
cortical bone > 170 MPa
2-12 MPa
trabecular bone
(d)
Elastic modulus (GPa)
Porosity (%)
cortical bone ≈ 20 GPa
0.1-5 GPa
trabecular bone
WE43 [69]
WE43+PEO
WE43 diamond [13]
JDBM biomimetic [54]
JDBM diamond
JDBM gyroid
Fe cubic [39]
Fe25Mn cubic
Fe35Mn Schwarz [38]
Fe diamond [14]
Zn diamond [45]
Zn diamond [12]
Zn diamond [42]
Zn+RGO diamond
Zn+2WE43 diamond [33]
Zn+5WE43 diamond
WE43 diamond [13]
JDBM biomimetic [54]
JDBM diamond
JDBM gyroid
Fe-35Mn Schwarz [38]
Fe diamond [14]
Zn diamond [45]
Zn diamond [12]
Zn diamond [42]
Zn+RGO diamond
Zn+2WE43 [33]
Zn+5WE43

Figure 2

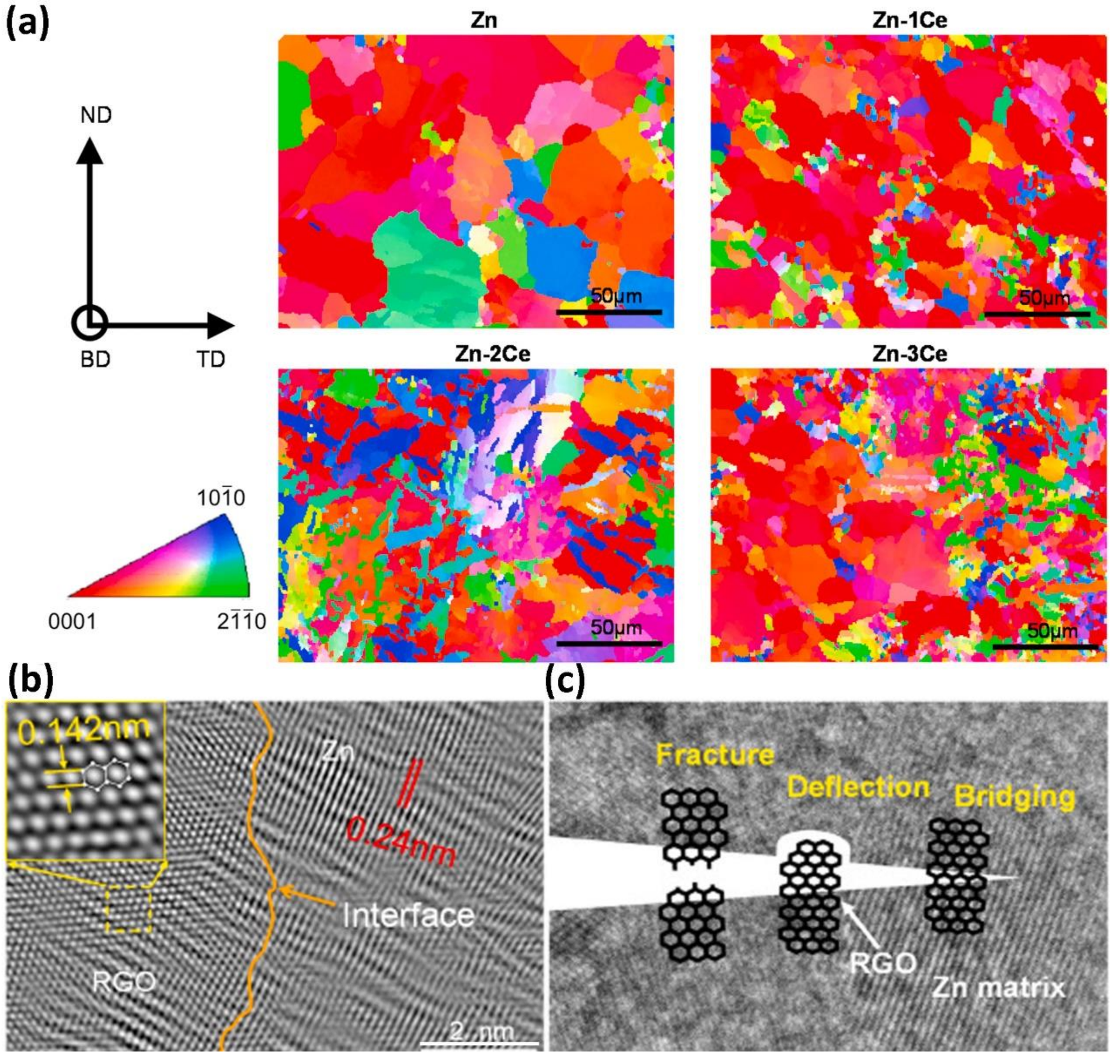

(a)
Zn
Zn-1Ce
Zn-2Ce
Zn-3Ce
ND
BD
TD
10$\bar{1}$0
0001
2$\bar{1}\bar{1}$0
50μm
50μm
50μm
50μm
(b)
0.142nm
Zn
0.24nm
Interface
RGO
2 nm
(c)
Fracture
Deflection
Bridging
RGO
Zn matrix

Figure 3

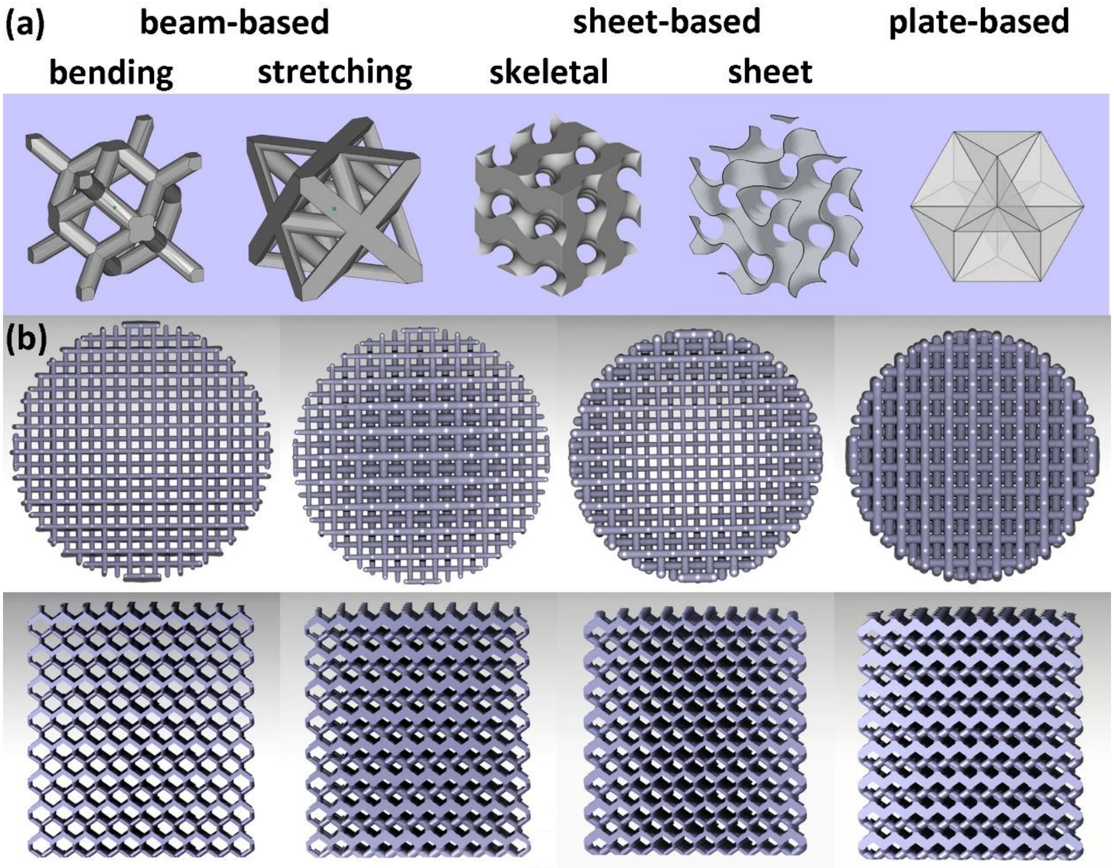
(a)
beam-based
sheet-based
plate-based
bending
stretching
skeletal
sheet
(b)

Figure 4

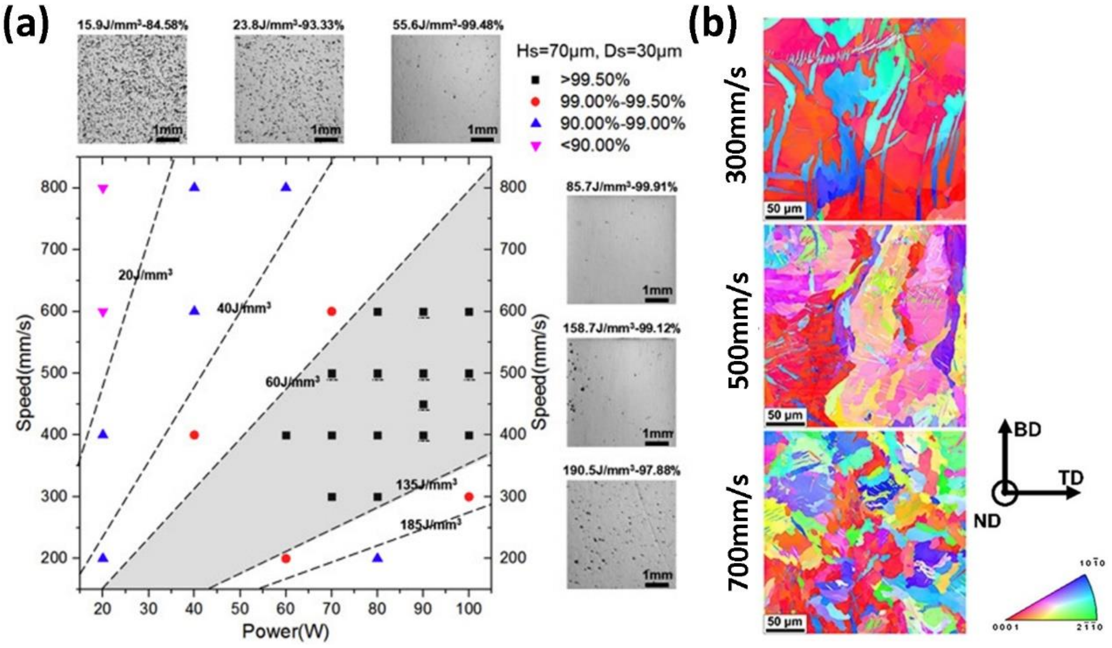

(a)
15.9J/mm³-84.58%
23.8J/mm³-93.33%
55.6J/mm³-99.48%
Hs=70μm, Ds=30μm
>99.50%
99.00%-99.50%
90.00%-99.00%
<90.00%
85.7J/mm³-99.91%
158.7J/mm³-99.12%
190.5J/mm³-97.88%
1mm
20J/mm³
40J/mm³
60J/mm³
135J/mm³
185J/mm³
Speed(mm/s)
Power(W)
(b)
300mm/s
500mm/s
700mm/s
50 μm
BD
TD
ND

Figure 5

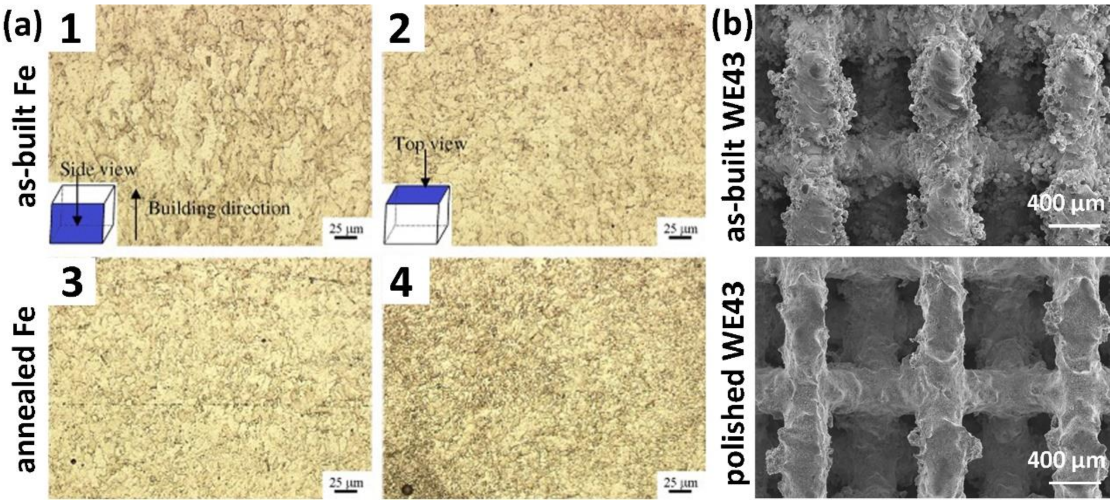

(a)
1
2
as-built Fe
Side view
Building direction
Top view
25 μm
25 μm
3
4
annealed Fe
25 μm
25 μm
(b)
as-built WE43
400 μm
polished WE43
400 μm

Table 1 The mechanical properties of AM biodegradable porous metals.

Material	Composition	Porosity %	Unit cell	Yield strength MPa	Elastic modulus GPa	Ultimate strength MPa	Ref.
cortical		3-5		170–193 (L*)	7–19 (L)		[15, 79]
				131 (T)	10-11 (T)		
					20-27 (R)		
trabecular		up to 90		2-12	0.1-5		
Mg	WE43	76	lattice			15	[74]
	WE43+PEO	70				31	
	WE43+PEO	76				23	
	WE43+PEO+HT	76				13	
	WE43	67	diamond	23	0.8	27	[13]
	JDBM	75	biomimetic	4.07	0.207		[56]
	JDBM	75	diamond	9.4	0.466		
	JDBM	75	gyroid	16.25	0.76		
Fe	Fe	67 ± 2	cubic	70 ± 4		135 ± 5	[41]
	Fe-25Mn	67 ± 2		137 ± 8		222 ± 11	
	Fe-35Mn	42	surface	89 ± 2	34 ± 2	304 ± 7	[40]
	Fe	85	diamond	11	1		[46]
		70		29	1		
		70		31	2		
		59		54	3		
	Fe	73	diamond	24	2		[14]
	Fe+HA			110	1		
Zn	Zn	73 ± 2	diamond	4	0.40		[47]
		69 ± 2	gradient	6	0.46		
		62 ± 3	diamond	11	0.79		
	Zn	75.8	diamond	11.7	0.76		[44]
	Zn+RGO	75.8	diamond	19.1	1.1		
	Zn+2WE43	67	diamond	50.9	1.9		[35]
	Zn+5WE43	67	diamond	66.2	2.48		
	Zn+8WE43	67	diamond	50.9	2.54		

* L, T, and R represent longitudinal, transverse, and random.